

Non-Equilibrium Phase Separation and Interface Dynamics in Active Systems

HARIKRISHNAN P S

*A dissertation submitted for the partial fulfilment
of BS-MS dual degree in Science*



Indian Institute of Science Education and Research Mohali
April 2017

THIS THESIS IS DEDICATED TO MY PARENTS

Certificate of Examination

This is to certify that the dissertation titled **Non-equilibrium Phase Separation and Interface Dynamics in Active Systems** submitted by **Harikrishnan P S** (Reg. No. MS11066) for the partial fulfillment of BS-MS dual degree programme of the Institute, has been examined by the thesis committee duly appointed by the Institute. The committee finds the work done by the candidate satisfactory and recommends that the report be accepted.

Dr. Sanjeev Kumar

Dr. Rajeev Kapri

Dr. Abhishek Chaudhuri

(Supervisor)

Dated: May 13, 2017

Declaration

The work presented in this dissertation has been carried out by me under the guidance of **Dr. Abhishek Chaudhuri** at the Indian Institute of Science Education and Research Mohali.

This work has not been submitted in part or in full for a degree, a diploma, or a fellowship to any other university or institute. Whenever contributions of others are involved, every effort is made to indicate this clearly, with due acknowledgement of collaborative research and discussions. This thesis is a bonafide record of original work done by me and all sources listed within have been detailed in the bibliography.

Harikrishnan P S

(Candidate)

Dated: May 13, 2017

In my capacity as the supervisor of the candidates project work, I certify that the above statements by the candidate are true to the best of my knowledge.

Dr. Abhishek Chaudhuri

(Supervisor)

Acknowledgment

First and foremost, I have to thank my parents and my sister for their love and support throughout my life.

I acknowledge my MS guide Dr. Abhishek Chaudhuri for his guidance and support throughout this study, and especially for his confidence in me.

I would like to thank Mr. Vipin Das for encouragement and guidance during all these years.

I also wish to express my gratitude to Dr. Anoop and Dr. Kavya Anoop.

I would never forget all the chats and beautiful moments I shared with some of my friends and classmates. They were fundamental in supporting me during stressful and difficult moments.

List of Figures

1.1	Examples of active matter systems	2
4.1	Phase separation in active colloid	20
5.1	Formation of active solid	21
5.2	Interface width as a function of time	22
5.3	Growth of interface for different lengths and for different Péclet numbers	23
5.4	Varitation of exponents with system size	24
5.5	Variation of exponents with Péclet number	25
5.6	Rescaled curves for different Péclet numbers	26

Abbreviations

BD	Ballistic Deposition
EW	Edwards - Wilkinson
KPZ	Kardar - Parisi - Zhang
RG	Renormalization Group

Abstract

Objective of this thesis work is to study the dynamics of an active interface. We performed parallel-molecular dynamic simulations for several system sizes and for different Péclet numbers on a minimal model for active systems. We have shown from numerical studies that this active colloidal system phase separates. We determined scaling exponents for the active solid-fluid interface (in $(1+1)$ dimensions), formed as a result of confining the active colloid system between two static boundaries. Results obtained indicates that the interface does not belong to the KPZ universality class.

Contents

1	Introduction	1
1.1	Active Matter	2
2	Brownian Motion	5
2.1	Smoluchowski Equation	5
2.2	Langevin Equation	7
3	Interface Dynamics	9
3.1	Ballistic Deposition	9
3.2	The Edwards-Wilkinson Equation	11
3.3	The KPZ Equation	12
3.4	Renormalization Group	13
3.5	Scaling Exponents for the KPZ Equation	13
4	Phase Separation in Active Colloids	17
4.1	Model and Simulation Method	17
4.2	Phase Separation	19
5	Confined Active Colloid	21
5.1	Active Solid	21
5.2	Active Solid-Fluid Interface	22
5.2.1	Dependence on System Size	22
5.2.2	Variation of Exponents with Peclet number	25
5.2.3	Rescaling	26
6	Summary	27
	Bibliography	30

Chapter 1

Introduction

Distinction between being “alive” or “not alive” has been a long-standing question in the scientific community. German philosopher Immanuel Kant was the first to define life as a self-organized, self-reproducing process. He distinguished living matter from non-living matter as self-organized processes. But understanding of self organized dynamic systems remained an open topic. According to second law of thermodynamics, natural choice of a system has to be a state with maximum entropy i.e. one with maximum disorder. Ordered states such as crystals in thermodynamics are static. In contrast living systems are open and energy flow through the system is used to reduce entropy and to generate order. In the new era living systems are redefined as dynamic organization emerges from the collective behavior of ‘agents’, the individual properties of which can not account for the properties of the final dynamic pattern.

Modelling living matter is a novel area of research. Active matter physics has arisen with the same motivation. Study of active systems is still at it’s infancy. Many emergent properties of active systems lack a complete explanation mainly due to their far from equilibrium nature.

In this project we present simulation and theory based studies of an active system using a minimal model of self-propelled Brownian disks interacting only via the excluded-volume repulsive potential. Aim of these studies is to characterize the dynamics and scaling properties of an active interface formed by these self-propelled Brownian particles.

1.1 Active Matter

Active particles contain internal degrees of freedom with the ability to take in and dissipate energy and, in the process, execute systematic movement [Ramaswamy 10]. Active matter systems composed of active particles span a wide range of length scales in nature, from elements of cytoskeleton to school of fishes to human stampedes. Some other examples for active matter systems are shown in Figure 1.1. These systems are not in thermodynamic equilibrium due to the requirement of constant throughput of energy, and are often far from equilibrium; therefore standard results of equilibrium thermodynamics and statistical mechanics do not apply.

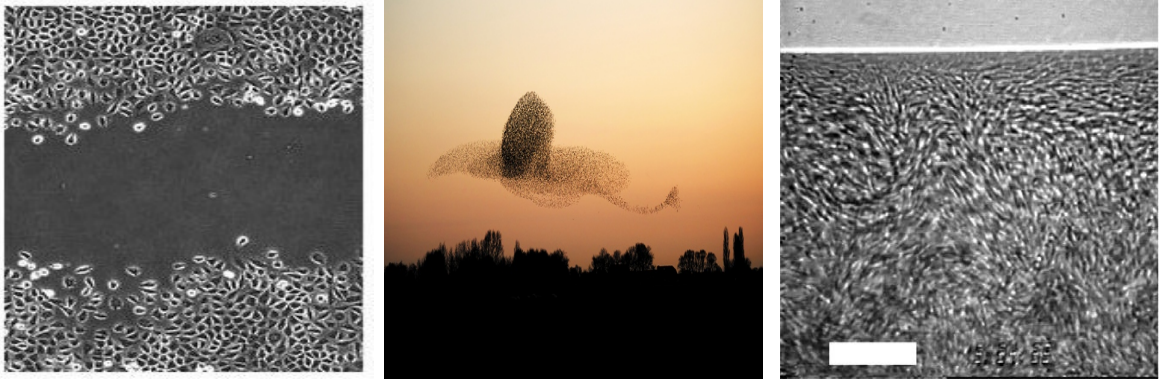


Figure 1.1: Examples of active matter systems. (left) Movement of fibroblast during wound healing [Steffen 13], (middle) Flock of starlings [Popkin 16], (right) Bacterial suspension [Hagan].

Active systems exhibit diverse properties such as self-motility, self-healing, internally generated flows, synchronous dynamics, etc. Pioneering work in the field of active matter belongs to Vicsek [Vicsek 95], he introduced a minimal model for active systems. Viscek model shows emergence of dynamic self organized state, starting from a disordered state. It has been used as a prototype model for different problems.

Several methods have been used to study active matter; including generalizations of theoretical techniques from statistical physics and condensed matter, as well as computer simulations and also laboratory experiments. Non-living synthetic self driven particles, called *Janus particles*, are also being used for the study of active systems.

Active colloids are mixtures in which microscopic self-propelled particles move through a viscous fluid by converting energy extracted from their environment. A signature property of these active colloids is the formation of dynamic self-assembled

states. Examples include tunable, self-healing colloidal crystals and membranes, self-assembled microswimmers, etc. Active Brownian particles provide a reasonably good starting point in modelling simple active colloidal systems. Numerical simulations on these simple model systems shows phase separation and formation of complex self-organized structures. Dynamic boundaries of these cluster states are fascinating and we have tried to characterize such an active interface formed in an active colloidal system.

Plan of Thesis

We have provided an introduction to Brownian dynamics and Langevin equation in chapter 2, which is fundamental requirement for the study of active colloids. Basic theories required for the study of active interface are discussed in chapter 3. We have introduced the Edwards-Wilkinson equation and KPZ equation for nonequilibrium interfaces in this chapter. Determination of scaling exponents using dynamic renormalization method is also included. Our model and simulation results are explained in chapter 4 and 5. Finally we summarize our results in chapter 6.

Chapter 2

Brownian Motion

The name Brownian motion is used to describe movement of particles suspended in a fluid. The phenomena was first reported by Scottish botanist Robert Brown in 1827. He was observing pollen grains suspended in water under a microscope and he noticed the jittery movement of particles ejected from pollen grains. But he was not able to come up with a satisfactory reason for the random movement of particles on water. Later in 1905, Albert Einstein provided a theoretical foundation for Brownian motion [Einstein 56], just by using thermodynamic principles and basic kinetic theory of gases.

2.1 Smoluchowski Equation

It is assumed that each particle moves independently of others and movements of individual particles are uncorrelated at different time steps. According to Fick's law, particle flux is proportional to spatial gradient of concentration,

$$J(x, t) = -D \frac{\partial f(x, t)}{\partial x} \quad (2.1)$$

where, J is particle flux, f concentration of particles and D is called the diffusion constant, which depends on system temperature and particle size,

$$D = \frac{k_B T}{\zeta} \quad (2.2)$$

where ζ is the friction constant. Equation (2.2) is known as Einstein's relation. For a spherical particle of radius a , in a fluid of viscosity η ,

$$\zeta = 6\pi\eta a \quad (2.3)$$

$f(x, t)$ has to obey the continuity equation, since number of particles in the system is fixed,

$$\frac{\partial f(x, t)}{\partial t} = -\frac{\partial J(x, t)}{\partial x} \quad (2.4)$$

Combining eqn (2.1) and eqn (2.4)

$$\frac{\partial f(x, t)}{\partial t} = D \frac{\partial^2 f(x, t)}{\partial x^2} \quad (2.5)$$

i.e. concentration of suspended particles in a fluid satisfies the diffusion equation, so $f(x, t)$ has to have the particular functional form given by,

$$f(x, t) = \frac{N}{\sqrt{4\pi Dt}} \exp\left(\frac{-x^2}{4Dt}\right) \quad (2.6)$$

This implies

$$\langle X(t)^2 \rangle = 2Dt \quad (2.7)$$

i.e. particles are spread out uniformly and the spread is proportional to the square root of time.

In presence of an external potential $U(x)$, particles will experience a force,

$$F = -\frac{\partial U(x)}{\partial x} \quad (2.8)$$

and the diffusion equation is modified,

$$\frac{\partial f(x, t)}{\partial t} = \frac{\partial}{\partial x} \frac{1}{\zeta} \left(k_B T \frac{\partial f}{\partial x} + f \frac{\partial U}{\partial x} \right) \quad (2.9)$$

Above equation is called the Smoluchowski equation.

This diffusion relation can be used to determine size of atoms and later for the experimental discovery of the same, J.B. Perrin was awarded the Nobel prize in 1926.

2.2 Langevin Equation

Time evolution of a free Brownian particle is best described by the Langevin equation,

$$m\dot{v} = -m\gamma v + \eta(t) \quad (2.10)$$

where m and v represent mass and instantaneous velocity of the Brownian particle, γ is a measure of drag force exerted by the fluid onto the particle (comparing with eqn.(2.3) $m\gamma = \zeta$). Brownian particles are constantly being bombarded by the fluid molecules, frequency of these collisions is very large (of the order of 10^{21} per second). This rules out possibility of a deterministic equation for the Brownian particles. In principle if we know position and velocity of all the fluid particles as a function of time, the force is uniquely determined. But, keeping track of all these rapidly varying forces is not a practical task. So, a stochastic variable η is introduced into the equation, representing fluctuations (called noise term). An assumption is that there exists a time interval $dt = t - t'$ such that $\eta(t)$ and $\eta(t')$ are uncorrelated, but during which a considerable change in v occurs.

$$\langle \eta(t) \rangle = 0 \quad (2.11)$$

$$\langle \eta(t)\eta(t') \rangle = \Gamma\delta(t - t') \quad (2.12)$$

where Γ determines strength of these fluctuations. Equation (2.11) implies that there is no preferred direction for the random force.

Mean square displacement of a particle satisfying the Langevin equation is given by,

$$\langle X(t)^2 \rangle = \frac{2k_B T}{m\gamma^2} [\gamma t - 1 + \exp(-\gamma t)] \quad (2.13)$$

At very long times, as $t \rightarrow \infty$, particle is in the diffusion regime and

$$\langle X(t)^2 \rangle = \frac{2k_B T}{m\gamma} t = 2Dt \quad (2.14)$$

From the Langevin equation, velocity auto-correlation function can be obtained,

$$\langle v(t)^2 \rangle = v(0)^2 e^{-2\gamma t} + \frac{\Gamma}{2m^2\gamma} [1 - e^{-2\gamma t}] \quad (2.15)$$

At long times system reaches equilibrium and mean square velocity is given by the Boltzmann distribution,

$$\langle v(t)^2 \rangle = \frac{k_B T}{m} \quad (2.16)$$

From eqn. (2.15) and eqn. (2.16),

$$\Gamma = 2m\gamma k_B T \quad (2.17)$$

It is the fluctuation-dissipation relation. It relates magnitude of fluctuations (Γ) to the strength of frictional force (γ) which causes dissipation.

In the presence of an external force F , Langevin equation becomes,

$$m\dot{v} = F - m\gamma v + \eta(t) \quad (2.18)$$

Chapter 3

Interface Dynamics

Formation and growth of interfaces depends upon many factors and writing down an explicit equation from the scratch is a formidable task. It is always better to look for a coarse grained equation, which describes the growth. The interesting fact about these interfaces is that they are generally self-affine fractals (i.e. invariant under anisotropic transformations), so it is possible to accommodate different models in the same universality class according to their scaling properties.

Below I've discussed scaling concepts and general approach in writing down a growth equation of an interface, focusing on the ballistic deposition model.

3.1 Ballistic Deposition

This simple model generates a nonequilibrium interface. In the lattice version of the BD model, a particle is released from a random position above the substrate, which vertically falls onto the substrate and sticks to the first encountered site, either to site directly below or to the nearest neighbor sites depending on their height with respect to the former.

In order to characterize the interface formed by deposition of particles, we define,

Mean height of the interface

$$\text{Mean height, } \bar{h}(t) = \frac{1}{L} \sum_{i=1}^L h(i, t) \quad (3.1)$$

where $h(i, t)$ is the height of i^{th} column at time t .

Interface Width

$$w(L, t) = \sqrt{\frac{1}{L} \sum_{i=1}^L [h(i, t) - \bar{h}(t)]^2} \quad (3.2)$$

$w(L, t)$ describes roughness of the interface at time t , w is a function of the lattice size.

Initially interface width shows a power law dependence in time. Time at which growth saturates and the saturation width, both depends on system size.

$$w(L, t) \sim t^\beta, \quad t \ll t_x \quad (3.3)$$

where t_x is the saturation time and β is called the *growth exponent*, which contains information about time dependent dynamics of the interface.

$$w_{sat}(L) \sim L^\alpha, \quad t \gg t_x \quad (3.4)$$

w_{sat} is the mean width of the saturated interface, α is the *roughness exponent*, it characterizes roughness of the saturated interface.

$$t_x \sim L^z \quad (3.5)$$

t_x is the saturation time and z is called the *dynamic exponent*.

In case of BD model, exponents α , β and z are not independent. They follow the Family-Vicsek scaling relation. Consequently, interface width has the following form,

$$w(L, t) \sim L^\alpha f\left(\frac{t}{L^z}\right) \quad (3.6)$$

where scaling function $f(u)$, $u = \frac{t}{t_x}$ [using eqn. (3.5)], has two domains

- For $t \gg t_x$, $u \gg 1$

In this region, according to eqn.(3.4), $f(u)$ should be a constant function.

- For $t \ll t_x$, $u \ll 1$

In this region, $f(u)$ is proportional to u^β ,

$$w(L, t) \sim L^\alpha u^\beta = L^\alpha \left(\frac{t^\beta}{L^{\beta z}} \right)$$

But, from eqn. (3.3), we require,

$$\alpha - \beta z = 0 \quad \Rightarrow \quad \frac{\alpha}{\beta} = z \quad (3.7)$$

This leads to the conclusion that any interface obeying scaling relation (3.6), the scaling exponents are related by equation (3.7).

3.2 The Edwards-Wilkinson Equation

Growth equation of interface for the BD model is assumed to have the following form,

$$\frac{\partial h(\mathbf{x}, t)}{\partial t} = G(h, \mathbf{x}, t) + \eta(\mathbf{x}, t) \quad (3.8)$$

where $h(\mathbf{x}, t)$ is interface height at time t at position \mathbf{x} . Gaussian white noise term $\eta(\mathbf{x}, t)$ denotes intrinsic random nature of the interface.

In order to find out explicit dependence of variables h , \mathbf{x} and t on G , we list out symmetries associated with the interface.

- Time translational symmetry
- Translational symmetry along the growth direction
- Translational symmetry perpendicular to the growth direction
- Rotational symmetry about the growth direction
- Symmetry about the mean interface height

(i), (ii) and (iii) rules out the explicit time, height and position dependence of G respectively. (iv) eliminates the possibility of odd order derivatives of h w.r.t. \mathbf{x} in G . Assuming that the interface is an equilibrium interface and there is no driving force along growth direction leads to (v). Neglecting higher order derivatives, the EW equation is given by,

$$\frac{\partial h(\mathbf{x}, t)}{\partial t} = v \frac{\partial^2 h}{\partial \mathbf{x}^2} + \eta(\mathbf{x}, t) \quad (3.9)$$

We know scaling relations obeyed by the BD interface, it can be used along with EW equation to determine values of the exponents. Since the interface is a self-affine fractal,

$$h(\mathbf{x}, t) = b^\alpha h(b\mathbf{x}, b^z t) \quad (3.10)$$

Under this rescaling, noise term is modified as,

$$\begin{aligned} \langle \eta(b\mathbf{x}, b^z t) \eta(b\mathbf{x}', b^z t') \rangle &= 2D \delta^d(b\mathbf{x} - b\mathbf{x}') \delta(b^z t - b^z t') \\ &= 2D \frac{1}{b^d} \delta^d(\mathbf{x} - \mathbf{x}') \frac{1}{b^z} \delta(t - t') \end{aligned} \quad (3.11)$$

thus, appropriate scaling for η is,

$$\eta(\mathbf{x}, t) = b^{(d+z)/2} \eta(b\mathbf{x}, b^z t) \quad (3.12)$$

Plugging (3.10) and (3.12) into (3.9) we obtain,

$$\begin{aligned} b^{\alpha-z} \frac{\partial h(b\mathbf{x}, b^z t)}{\partial t} &= v b^{\alpha-2} \frac{\partial^2 h(b\mathbf{x}, b^z t)}{\partial \mathbf{x}^2} + b^{-(d+z)/2} \eta(\mathbf{x}, t) \\ \Rightarrow \frac{\partial h(b\mathbf{x}, b^z t)}{\partial t} &= v b^{z-2} \frac{\partial^2 h(b\mathbf{x}, b^z t)}{\partial \mathbf{x}^2} + b^{-\alpha-d/2+z/2} \eta(\mathbf{x}, t) \end{aligned} \quad (3.13)$$

Since the interface is invariant under this transformation, exponents are given as,

$$\alpha = \frac{2-d}{2}, \beta = \frac{2-d}{4}, z = 2 \quad (3.14)$$

According to EW equation, 1-dimensional BD model is included in the universality class having $\alpha = 0.5$, $\beta = 0.25$ and $z = 2$.

However, values of exponents obtained from numerical simulations for the BD model are different from analytical predictions of EW equation. This discrepancy is resolved in the KPZ equation by introducing non-linear terms into EW equation. KPZ equation and dynamic RG method are discussed in the following section.

3.3 The KPZ Equation

KPZ equation, named after Mehran Kardar, Giorgio Parisi and Yi-Cheng Zang[Kardar 86], is a stochastic partial differential equation describing the evolution of a growing interface(3.15). It introduces a non-linear term to the EW equation. In the BD model, lateral growth is possible and this adds a non-linear term to the component of velocity

along the direction of overall growth.

$$\frac{\partial h(\mathbf{x}, t)}{\partial t} = v \frac{\partial^2 h}{\partial x^2} + \frac{\lambda}{2} \left(\frac{\partial h}{\partial x} \right)^2 + \eta(\mathbf{x}, t) \quad (3.15)$$

Interface has a non-zero mean velocity,

$$\nu = \frac{\lambda}{2} \int_0^L d^d \mathbf{x} \left\langle \left(\frac{\partial h}{\partial x} \right)^2 \right\rangle \quad (3.16)$$

If we apply the scaling procedure used for the EW equation, we ran into trouble, because here the parameters v , λ and D are not independent, they are coupled to each other. So we have to find out the relationship between these parameters and use a method called dynamic renormalization group to figure out the correct scaling exponents.

3.4 Renormalization Group

Renormalization group is a mathematical tool to investigate changes of a physical system during a scale transformation. Consider a system which is in a particular state, described by parameters, say a, b, c $[S(a, b, c)]$. Now we rescale the system in energy/length or in some other parameter. If we can represent new state of the system using the same set of variables $[S'(a', b', c')]$ then the system is said to be renormalizable. In case of non-renormalizable systems rescaling requires additional parameters to specify emerged state. Repeated application of RG transformation on a system can lead to fixed points in parameter space. And thereby allowing to identify scaling exponents.

3.5 Scaling Exponents for the KPZ Equation

For a stochastic equation we have to use the generalized dynamic renormalization group method to determine fixed points.

In the first step, we expand the KPZ equation in Fourier space in powers of λ and calculate first order corrections to the parameters $(\tilde{v}, \tilde{\lambda}, \tilde{D})$.

(Note : only main steps involved are discussed, long calculations involving integrals

are skipped)

Upon rescaling the KPZ equation, we obtain,

$$\frac{\partial h}{\partial t} = vb^{z-2}\frac{\partial^2 h}{\partial x^2} + \frac{\lambda}{2}b^{z+\alpha-2}\left(\frac{\partial h}{\partial x}\right)^2 + b^{-d/2+z/2-\alpha}\eta \quad (3.17)$$

Fourier Transforming (3.15) gives,

$$-i\omega h(\mathbf{k}, \omega) = -v\mathbf{k}^2 h(\mathbf{k}, \omega) - \frac{\lambda}{2} \int \int \left[\frac{d^d \mathbf{q} d\Omega}{(2\pi)^{d+1}} \mathbf{q} \cdot (\mathbf{k} - \mathbf{q}) h(\mathbf{q}, \Omega) h(\mathbf{k} - \mathbf{q}, \omega - \Omega) \right] \quad (3.18)$$

In momentum space, \mathbf{k} has an upper cut-off $\Lambda = \frac{2\pi}{\mathbf{a}}$, where \mathbf{a} is lattice spacing in real space.

Rearranging and defining $G_0(\mathbf{k}, \omega) = \frac{1}{v\mathbf{k}^2 - i\omega}$ we obtain,

$$h(\mathbf{k}, \omega) = G_0(\mathbf{k}, \omega)\eta(\mathbf{k}, \omega) - \frac{\lambda}{2}G_0(\mathbf{k}, \omega) \int \int \left[\frac{d^d \mathbf{q} d\Omega}{(2\pi)^{d+1}} \mathbf{q} \cdot (\mathbf{k} - \mathbf{q}) h(\mathbf{q}, \Omega) h(\mathbf{k} - \mathbf{q}, \omega - \Omega) \right] \quad (3.19)$$

Going from (3.18) to (3.19), it is assumed that noise is uncorrelated in the reciprocal space.

When $\lambda = 0$, we have,

$$h(\mathbf{k}, \omega) = G_0(\mathbf{k}, \omega)\eta(\mathbf{k}, \omega) \quad (3.20)$$

We define, for $\lambda \neq 0$

$$h(\mathbf{k}, \omega) \equiv G(\mathbf{k}, \omega)\eta(\mathbf{k}, \omega) \quad (3.21)$$

Now, equation (3.19) becomes,

$$\begin{aligned} G(\mathbf{k}, \omega)\eta(\mathbf{k}, \omega) &= G_0(\mathbf{k}, \omega)\eta(\mathbf{k}, \omega) - \frac{\lambda}{2}G_0(\mathbf{k}, \omega) \int \int \left[\frac{d^d \mathbf{q} d\Omega}{(2\pi)^{d+1}} \mathbf{q} \cdot (\mathbf{k} - \mathbf{q}) \right. \\ &\quad \left\{ G_0(\mathbf{q}, \omega)G_0(\mathbf{k} - \mathbf{q}, \omega - \Omega)\eta(\mathbf{q}, \omega)\eta(\mathbf{k} - \mathbf{q}, \omega - \Omega) \right. \\ &\quad \left. - \frac{\lambda}{2}G_0(\mathbf{q}, \Omega)G_0(\mathbf{k} - \mathbf{q}, \omega - \Omega)\eta(\mathbf{q}, \Omega) \right. \\ &\quad \int \int \left[\frac{d^d \mathbf{q}'' d\Omega''}{(2\pi)^{d+1}} \mathbf{q}'' \cdot (\mathbf{q}' - \mathbf{q}'')G_0(\mathbf{q}'', \Omega'')\eta(\mathbf{q}'', \Omega'') \right. \\ &\quad \left. - \frac{\lambda}{2}G_0(\mathbf{q}, \Omega)G_0(\mathbf{k} - \mathbf{q}, \omega - \Omega)\eta(\mathbf{k} - \mathbf{q}, \omega - \Omega) \right. \\ &\quad \left. \left. \int \int \frac{d^d \mathbf{q}' d\Omega'}{(2\pi)^{d+1}} \mathbf{q}' \cdot (\mathbf{q} - \mathbf{q}')G_0(\mathbf{q}', \Omega')\eta(\mathbf{q}', \Omega') + O(\lambda)^2 \right\} \right] \end{aligned} \quad (3.22)$$

In order to eliminate η from the above equation, we multiply both sides with $\eta(-\mathbf{k}, -\omega)$ and average over all space. So, terms with odd number of η are averaged to zero and others will lead to delta functions, since,

$$\langle \eta(\mathbf{k}, \omega) \rangle = 0 \quad (3.23)$$

$$\langle \eta(\mathbf{k}, \omega) \eta(\mathbf{k}', \omega') \rangle = 2D(2\pi)^d \delta^d(\mathbf{k} + \mathbf{k}') \delta(\omega + \omega') \quad (3.24)$$

Resulting equation for $G(\mathbf{k}, \omega)$ is,

$$G(\mathbf{k}, \omega) = G_0(\mathbf{k}, \omega) + 4 \left(\frac{-\lambda}{2} \right)^2 2D G_0^2(\mathbf{k}, \omega) \int \int \frac{d^d \mathbf{q} d\Omega}{(2\pi)^{d+1}} (-\mathbf{q}\mathbf{k}) \cdot \mathbf{q}(\mathbf{k} - \mathbf{q}) \quad (3.25)$$

$$G_0(\mathbf{k} - \mathbf{q}, \omega - \Omega) G_0(\mathbf{q}, \Omega) G_0(-\mathbf{q}, -\Omega + O(\lambda^4))$$

After carrying out integration, in the hydrodynamics limit (i.e. $t \rightarrow \infty$ and $a \rightarrow \infty$) we obtain,

$$G(\mathbf{k}, 0) = G_0(\mathbf{k}, 0) + \frac{\lambda^2 D}{v^2} G_0^2(\mathbf{k}, 0) \frac{d-2}{4d} k^2 K_d \int dq q^{d-3} \quad (3.26)$$

where,

$$K_d = \frac{S_d}{(2\pi)^d}, \quad S_d \text{ is the surface area of d-dimensional unit sphere} \quad (3.27)$$

Using the definition of $G_0(\mathbf{k}, \omega)$ and defining $G(\mathbf{k}, 0) = \frac{1}{\tilde{v}k^2}$, we obtain perturbative correction to v ,

$$\tilde{v} = v \left[1 - \frac{\lambda^2 D}{v^3} \frac{d-2}{4d} K_d \int dq q^{d-3} \right] \quad (3.28)$$

Similarly we can find corrections to λ and D and it comes out to be ,

$$\tilde{\lambda} = \lambda \quad (3.29)$$

$$\tilde{D} = D \left[1 + \frac{\lambda^2 D}{v^3} \frac{K_d}{4} \int dq q^{d-3} \right] \quad (3.30)$$

Perturbatively expanding second term in equation (3.19) will give correction to λ and from eqn.(3.24) correction to D can be obtained. These corrected parameters satisfy the scaling relation given in equation (3.17).

Next step is to apply RG transformation to these variables and calculate the exponents. Here \mathbf{k} values range from 0 to Λ .

- In step 1 of RG fast modes with $e^{-l} < |\mathbf{k}| < \Lambda$ (where $b \equiv e^{-l}$) are integrated out.
- Parameters are then rescaled as $\mathbf{k}' = e^{-l}\mathbf{k}$, $t' = e^{-zl}t$ and $h'(\mathbf{k}', t') = e^{-\alpha l}h(\mathbf{k}, t)$ in step 2.

This procedure will lead to the following flow equations,

$$\frac{dv}{dl} = v \left[z - 2 + K_d \bar{\lambda}^2 \frac{2-d}{4d} \right] \quad (3.31)$$

$$\frac{dD}{dl} = D \left[z - d - 2\alpha + K_d \frac{\bar{\lambda}^2}{4} \right] \quad (3.32)$$

$$\frac{d\lambda}{dl} = \lambda [\alpha + z - 2] \quad (3.33)$$

where $\bar{\lambda} = \lambda^2 D / v^3$ is the coupling constant.

Equation (3.34) immediately gives the relation between α and z ,

$$\alpha + z = 2 \quad , \quad \text{independent of dimension} \quad (3.34)$$

We can obtain the flow of coupling constant using (3.31), (3.32) and (3.34)

$$\frac{d\bar{\lambda}}{dl} = \frac{2-d}{2} \bar{\lambda} + K_d \frac{2d-3}{4d} \bar{\lambda} \quad (3.35)$$

In one dimensional case, non-zero fixed point of $\bar{\lambda}$ is

$$\bar{\lambda}^* = \left(\frac{2}{K_d} \right)^2 \quad (3.36)$$

Substituting (3.36) in (3.31) and (3.32), we obtain,

$$z = \frac{3}{2} \quad \alpha = \frac{1}{2} \quad (3.37)$$

These are exact scaling exponents for the BD model in 1D. From equation (3.7),

$$\beta = \frac{1}{3} \quad (3.38)$$

Chapter 4

Phase Separation in Active Colloids

This chapter includes simulation and theory based studies of a minimal model of active particles. This active colloidal system phase separates into a solid region and a fluid region as activities of individual particles are increased. We have successfully reproduced this characteristic behavior of active systems.

4.1 Model and Simulation Method

Our model consists of self-propelled smooth disks immersed in a fluid and confined to a plane [Redner 13]. Particles interact with each other via the excluded volume potential only. No mutual alignment interactions are explicitly included.

Position(r_i) and self-propulsion direction(θ_i) of particles completely specify state of the system. Time evolution of particles is governed by the coupled overdamped Langevin equations,

$$\dot{r}_i = D\beta[F_{ex}(r_i) + F_p\hat{\mathbf{v}}_i] + \sqrt{2D}\eta_i^T \quad (4.1)$$

$$\dot{\theta}_i = \sqrt{2D_r}\eta_i^R \quad (4.2)$$

where, $F_{ex}(r) = -\frac{dU_{ex}(r)}{dr}$.

$U_{ex}(r)$ is called the WCA potential, given by,

$$U_{ex}(r) = \begin{cases} 4\epsilon \left[\left(\frac{\sigma}{r}\right)^{12} - \left(\frac{\sigma}{r}\right)^6 \right] + \epsilon & \text{if } r < 2^{\frac{1}{6}} \\ 0 & \text{otherwise} \end{cases} \quad (4.3)$$

σ is particle diameter, $\epsilon = k_B T$.

D and D_r are translational and rotational diffusion coefficients. In the low Reynolds number [Purcell 77] (a dimensionless parameter that compares the effect of inertial and viscous forces) regime, i.e. in the overdamped regime, they are related as,

$$D_r = \frac{3D}{\sigma^2} \quad (4.4)$$

Since particles are being driven continuously with an external source of energy, there exist a constant throughput of energy into the system. This makes the system intrinsically out of equilibrium. F_p is the constant driving force on particles (self-propulsion force), F_p is not derivable from any potential. Action of F_p on a particle will move it with a velocity,

$$\mathbf{v}_p = D\beta F_p \hat{\mathbf{v}}_i \quad (4.5)$$

where,

$$\hat{\mathbf{v}}_i = \begin{pmatrix} \cos \theta_i \\ \sin \theta_i \end{pmatrix}, \quad \beta = \frac{1}{k_B T} \quad (4.6)$$

η are the uncorrelated Gaussian noise,

$$\langle \eta \rangle = 0 \quad \text{and} \quad \langle \eta_i(t) \eta_j(t') \rangle = 2D \delta_{ij} \delta(t - t') \quad (4.7)$$

Equations of motion are non-dimensionalized using σ , $k_B T$ and $\tau = \frac{\sigma^2}{D}$ as basic units of length, energy and time respectively. The system is parametrised by two functions, system density ρ ($\rho = \frac{N^2}{L^2}$, where N is number of particles in the system and L is system length) and the Péclet number Pe ¹. In this system Péclet number is same as the non-dimensionalized self-propulsion velocity,

$$Pe = \frac{v_p \tau}{\sigma} \quad (4.8)$$

We employed molecular dynamics simulation technique to integrate the equations of motion. Integration of stochastic equations (4.1 and 4.2) were established using the stochastic Euler scheme. Time constraint was one of the major difficulty we have encountered during execution. For a system of N particles, calculation of resultant

¹Péclet number is defined as ratio of bulk flow of a quantity to rate of diffusion of the same quantity,

$$Pe = \frac{\text{rate of advection}}{\text{rate of diffusion}}$$

potential on a single particle requires time-steps of the order of N^2 . Parallel programming techniques using OpenMP [Hermanns 02] were used to reduce simulation time for calculating pair-wise interactions. We have successfully been able to reduce this exponential time requirement by threading the loops.

4.2 Phase Separation

Despite the absence of mutual aligning interactions, the system undergoes nonequilibrium clustering. Similar to an equilibrium system undergoing phase separation in presence of attractive interactions, system phase separates here with system activity Pe as the control parameter. As a reason, the starting fluid phase eventually leads to a system with solid-fluid coexistence.

We employ simulations on a system with 4096 particles with average particle density 0.8 (corresponding system length is 70) for Pe values 10, 50, 90 and 150. Simulations were carried out for $2 \times 10^6 dt$, where $dt = 10^{-5}$, and collected data at regular intervals after the system had reached steady-state. In this simulation we have waited for the first 1×10^{-6} time-steps for the system to reach steady-state.

Obtained results are shown in Figure 5.1. For $Pe = 10$, system is in the single phase region and the density distribution is peaked about the overall system density 0.8. i.e. for small Péclet numbers there is no particle accumulation in the system. Density distribution broadens out as particles start clustering due to the increased activity in the system. Further increase in system activity leads to phase separation (two distinct densities can be seen for $Pe = 150$). This shows coexistence of solid and fluid phases for larger Péclet numbers. Emergence of this non-intuitive phase separation behavior is a signature of active fluids, as it has been observed in other active system models. These observations suggest that, apart from achieving a density larger than the critical density, the system requires a minimum activity in order for cluster formation.

It has been shown that the dense phase exhibits structural signatures of a crystalline solid near crystal-hexatic transition point and anomalous dynamics including superdiffusive motion on intermediate time scales [Redner 13]. A microscopic theory for the phase separation of self-propelled repulsive disks has been introduced by Bialké, Löwen and Speck [Buttinoni 13].

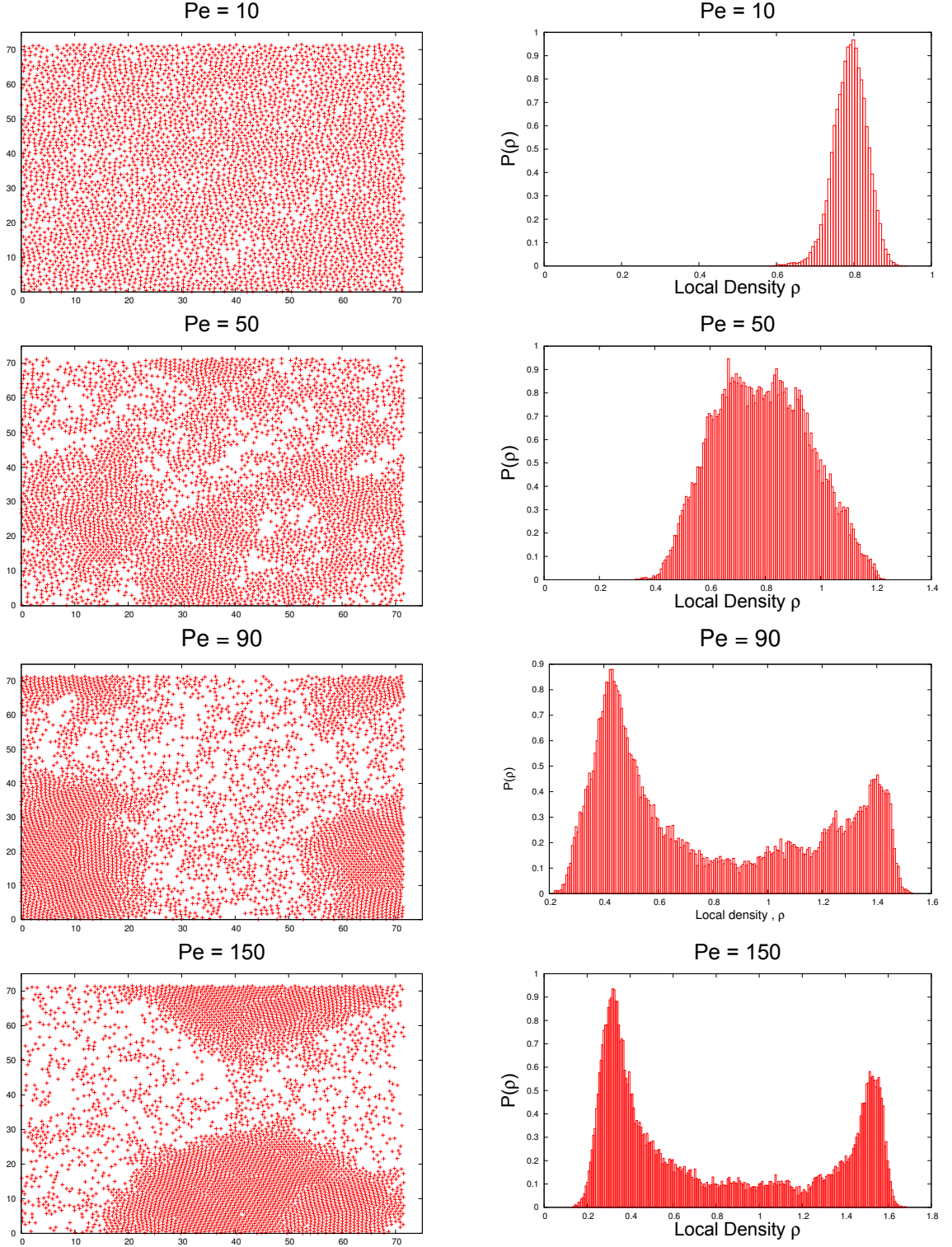


Figure 4.1: (left) snapshot of the system configuration for different Pe (right) corresponding local density distributions. Distribution corresponding to the single density broadens and flattens as Pe is increased and becomes binodal as the system phase separates. $N = 4096$, $L = 70$, Average density = 0.80, Time-steps = $20 \times 10^5 dt$.

Chapter 5

Confined Active Colloid

5.1 Active Solid

Confining the active colloidal system discussed in chapter 4 between two static boundaries causes particle accumulation at the boundaries (Figure 5.1). This dense phase has the characteristic properties of a 2D colloidal crystal [Redner 13] and is given the name “active solid”. Formation of active solid separates the system into a solid phase at the boundaries and a fluid phase in between.

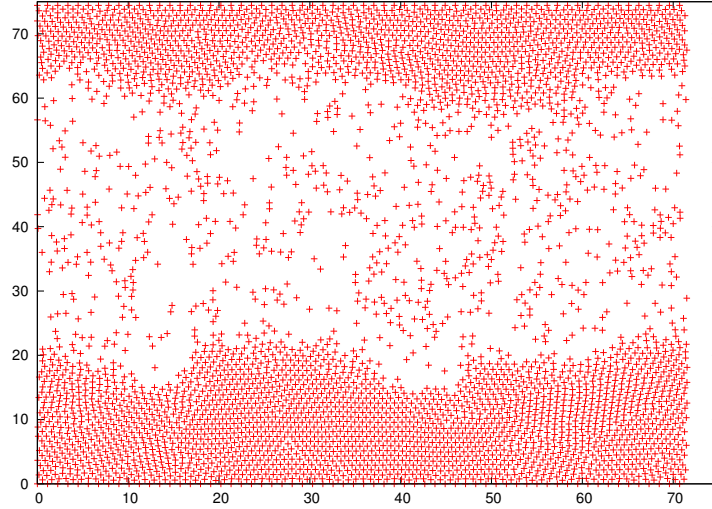


Figure 5.1: Accumulation of particles at the boundaries, leaving a fluid region in the center. ($N = 4096$, $L = 70$, Snapshot of system after 10^6 time-steps)

5.2 Active Solid-Fluid Interface

Time evolution of this active solid-fluid interface shows same characteristics as that of a BD interface. The interface grows as a power law in time before saturating (Figure 5.2). In order to determine scaling exponents and the universality class to which the interface belong, we have done simulations for different system sizes 70,80,90,100,110,120,130 and 150 (corresponding to 4096, 5184, 6400, 8100, 10000, 12100, 13225 and 18225 particles respectively) and for different Péclet numbers (100, 115, 135 and 150).

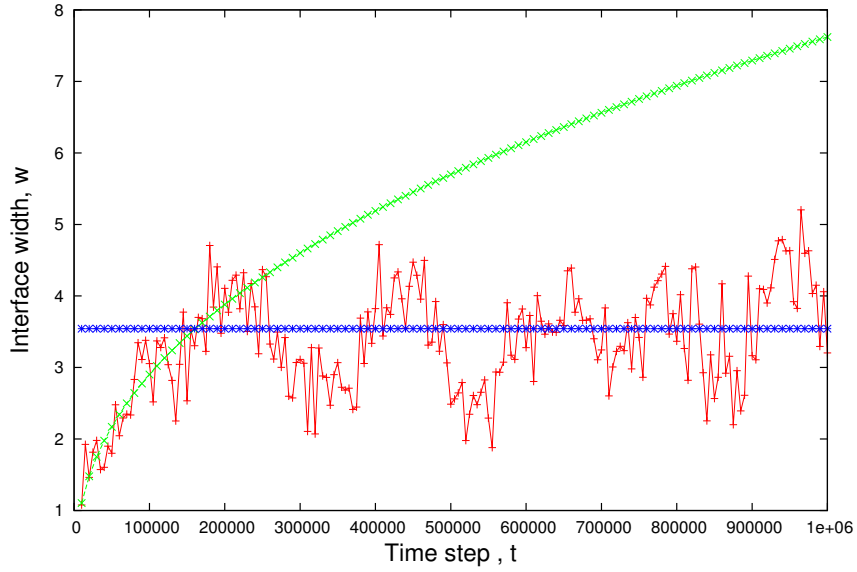


Figure 5.2: Growth of interface width as a function of time for an active solid-fluid interface ($L = 70$, $N = 4096$). Green line shows initial t^β dependence and blue line corresponds to the mean saturated width. Point of intersection of these lines give the crossover time t_x .

5.2.1 Dependence on System Size

Plots for interface width as a function of time for different lengths and for different Péclet values are shown in (Figure 5.3). From these simulations have obtained values for beta, saturation width and saturation time for different system sizes. In Figure 5.4 we plot them as a function of system size for a given Péclet number ($Pe = 150$).

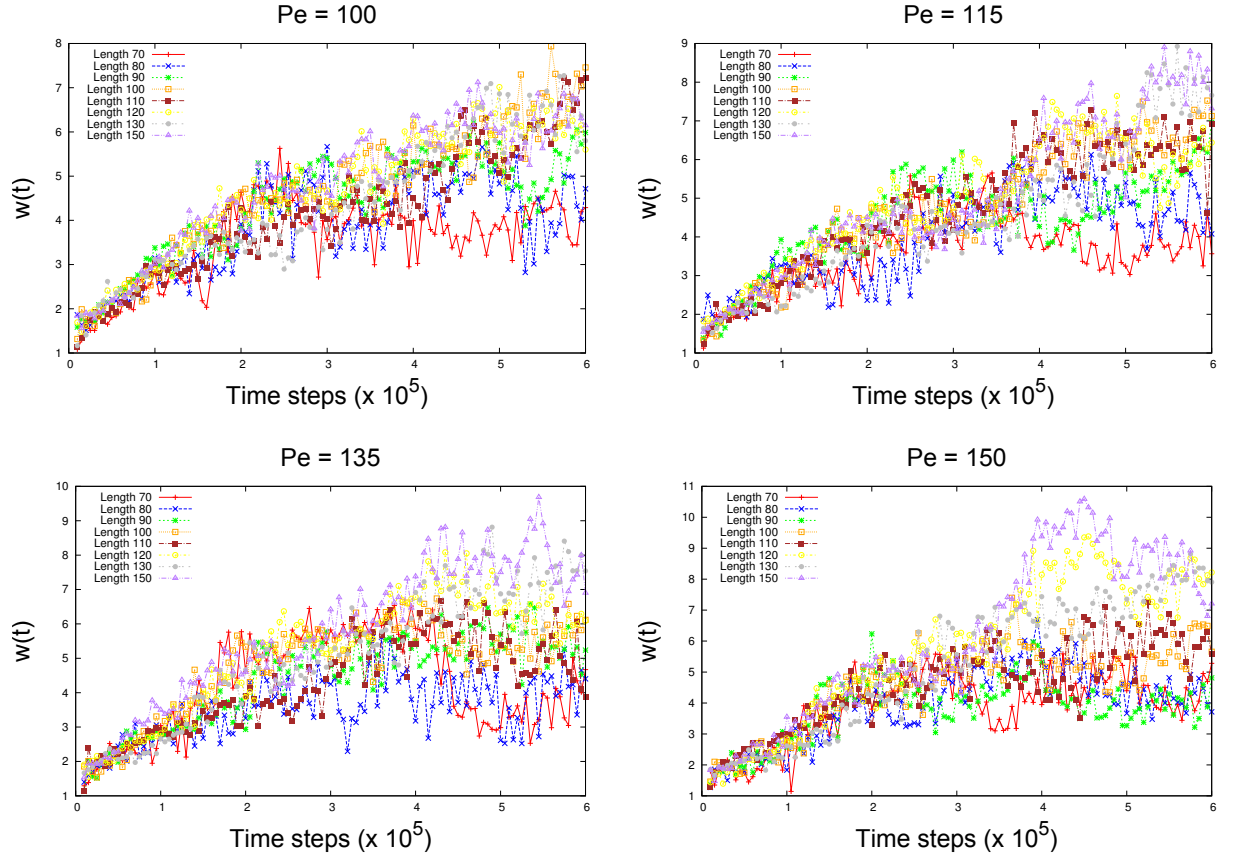


Figure 5.3: Growth of interface for different lengths and for different Péclet numbers

Observations from Figure 5.3 and Figure 5.4 suggest that the growth exponent β is independent of system size whereas mean saturation width (w_{sat}) and saturation time (t_x) follows a power law in length. At this point it is reasonable to assume that scaling behavior of this active interface has same characteristics that of a BD interface. i.e.

$$\begin{aligned}
 w &\sim t^\beta \quad \text{for } t < t_x \\
 w_{sat} &\sim L^\alpha \quad \text{for } t > t_x \quad \text{and} \\
 t_x &\sim L^z
 \end{aligned}$$

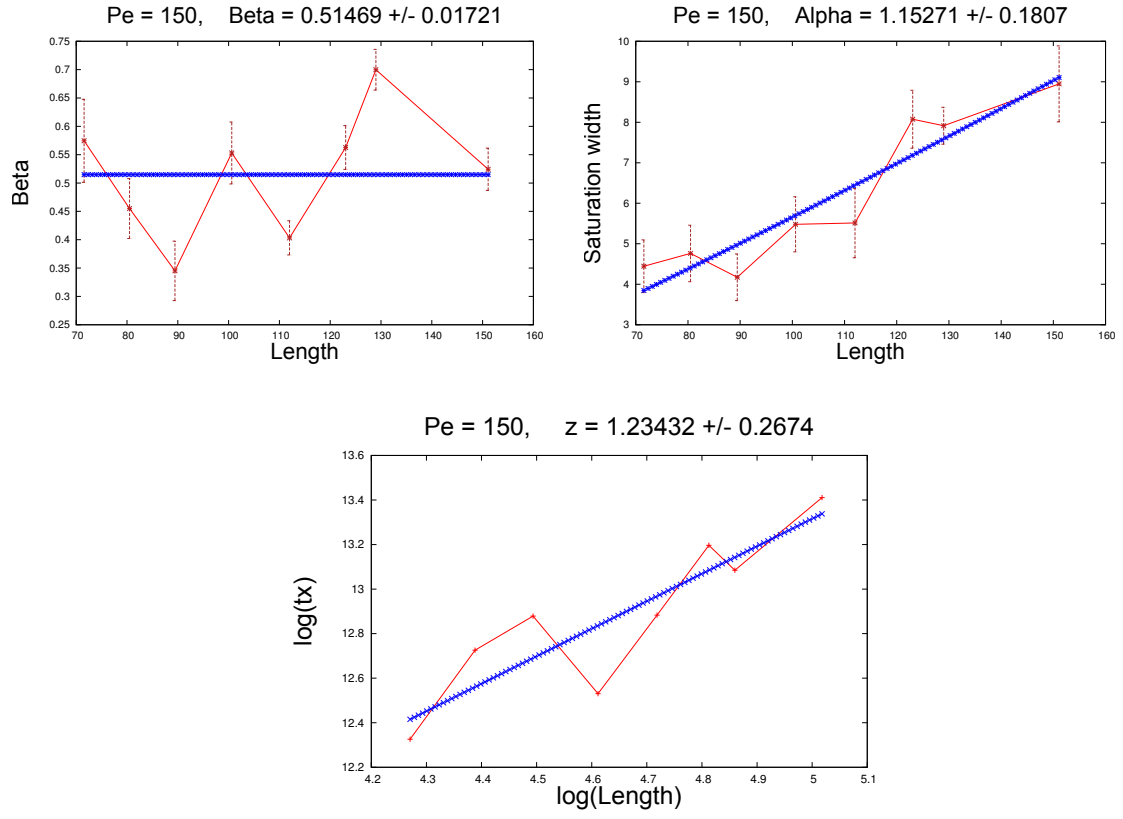


Figure 5.4: Variation of exponents with system size

5.2.2 Variation of Exponents with Peclet number

From simulations we have determined scaling exponents (α , β and z) for different Péclet numbers. Variations of these exponents as a function of system activity are given below.

Roughness exponent increases as activity in the system increases. This implies that

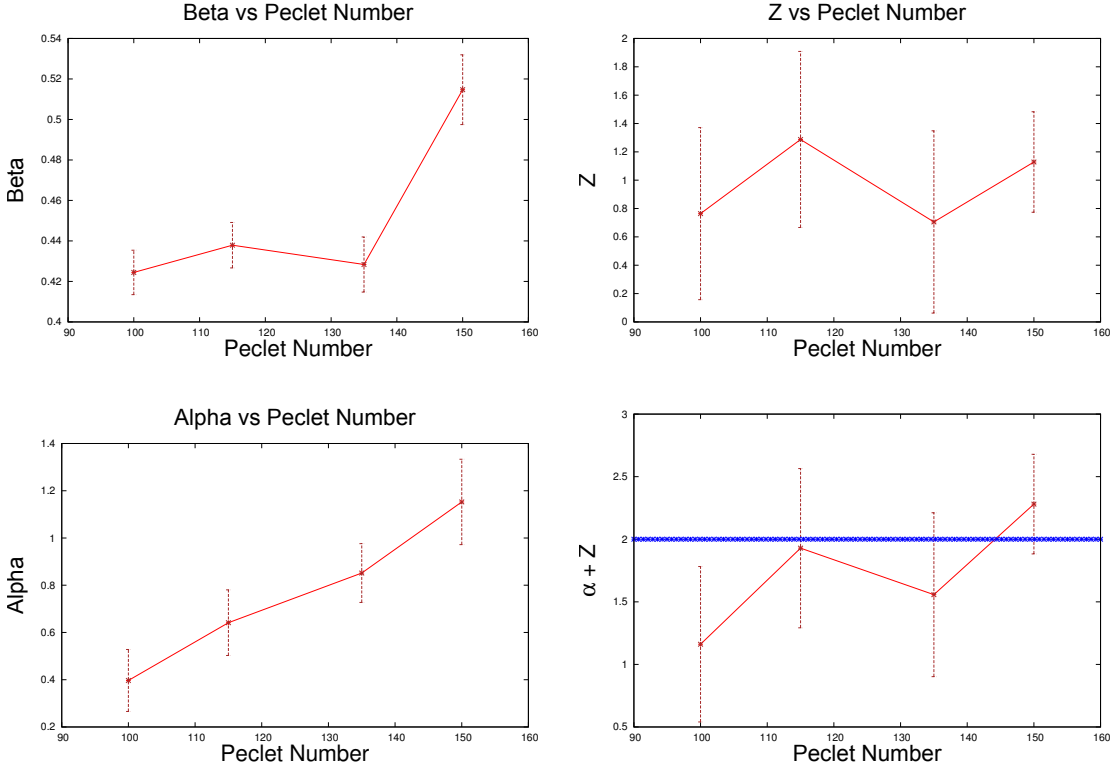


Figure 5.5: Top left : Variation of roughness exponent with Pe . Top right : Beta as a function of Pe . Bottom left : Variation of Z with Pe . Bottom right : Variation of $\alpha + z$ with Pe , blue line is the KPZ equation prediction

roughness of the interface is determined by activity in the system. We plotted the value of $\alpha + z$ for different Pe values, in order to find out whether this interface belong to the KPZ universality class. For KPZ interface, value of $\alpha + z = 2$, independent of interface dimensions (equation 3.34).

5.2.3 Rescaling

In order to figure out whether the interface follows any scaling relation, we rescaled the curves. Shown below are the rescaled curves corresponding to different system activities. Horizontal axis is rescaled with L^z and vertical axis with L^α .

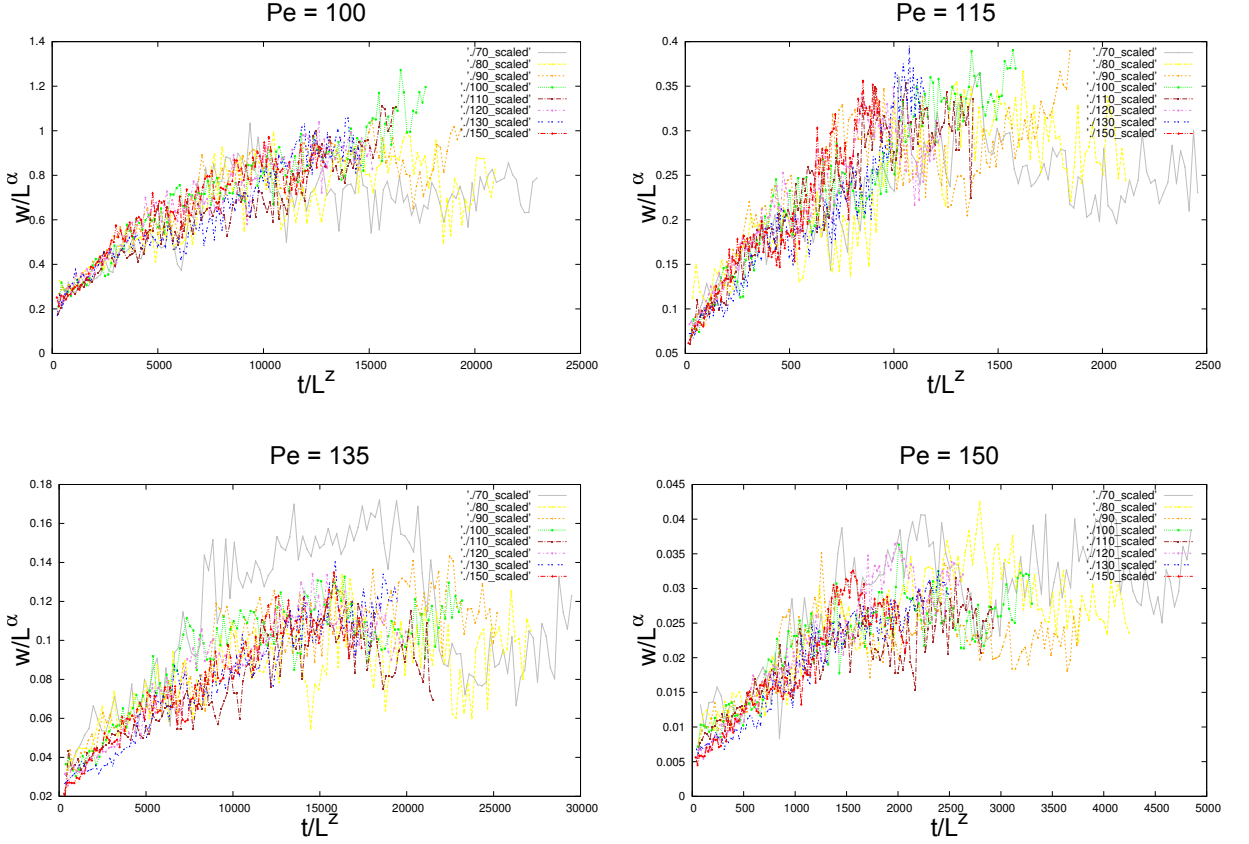


Figure 5.6: Rescaled curves for different Péclet numbers

Chapter 6

Summary

We started with a minimal model for active systems and showed the existence of dynamic self organization in the system. System phase separated into a solid-fluid phase as we increase self propulsion velocities of individual particles. Later we showed the formation of a solid phase near boundaries once the system is confined between two static boundaries. Our focus was on the active interface formed by the active solid in the system. We couldn't find conclusive evidences to assure that the interface is governed by the KPZ equation. We have to do simulations for larger system sizes in order to obtain better results.

All codes, graphs and animations can be found here ‘ https://github.com/MSTHESIS/Active_Matter ’

Bibliography

- [Barabási 95] A-L Barabási & Harry Eugene Stanley. Fractal concepts in surface growth. Cambridge university press, 1995.
- [Buttinoni 13] Ivo Buttinoni, Julian Bialké, Felix Kümmel, Hartmut Löwen, Clemens Bechinger & Thomas Speck. *Dynamical clustering and phase separation in suspensions of self-propelled colloidal particles*. Physical review letters, vol. 110, no. 23, page 238301, 2013.
- [Chandrasekhar 43] Subrahmanyan Chandrasekhar. *Stochastic problems in physics and astronomy*. Reviews of modern physics, vol. 15, no. 1, page 1, 1943.
- [Einstein 56] Albert Einstein. Investigations on the theory of the brownian movement. Courier Corporation, 1956.
- [Fily 12] Yaouen Fily & M Cristina Marchetti. *Athermal phase separation of self-propelled particles with no alignment*. Physical review letters, vol. 108, no. 23, page 235702, 2012.
- [Frenkel 01] Daan Frenkel & Berend Smit. Understanding molecular simulation: from algorithms to applications, volume 1. Academic press, 2001.
- [Hagan] Michael Hagan. *A bacterial suspension*. <https://www.brandeis.edu/departments/physics/hagan/research/activematter.html>.
- [Hermanns 02] Miguel Hermanns. *Parallel programming in Fortran 95 using OpenMP*. Universidad Politecnica de Madrid, Spain, 2002.

- [Kardar 86] Mehran Kardar, Giorgio Parisi & Yi-Cheng Zhang. *Dynamic scaling of growing interfaces*. Physical Review Letters, vol. 56, no. 9, page 889, 1986.
- [Popkin 16] Gabriel Popkin. *The physics of life*, Jan 5, 2016.
- [Purcell 77] Edward M Purcell. *Life at low Reynolds number*. American journal of physics, vol. 45, no. 1, pages 3–11, 1977.
- [Ramaswamy 10] Sriram Ramaswamy. *The mechanics and statistics of active matter*. Annu. Rev. Condens. Matter Phys., vol. 1, no. 1, pages 323–345, 2010.
- [Redner 13] Gabriel S Redner, Michael F Hagan & Aparna Baskaran. *Structure and dynamics of a phase-separating active colloidal fluid*. Physical review letters, vol. 110, no. 5, page 055701, 2013.
- [Steffen 13] et. al. Steffen. *Rac function is crucial for cell migration but is not required for spreading and focal adhesion formation*. J Cell Sci, vol. 126, no. 20, pages 4572–4588, 2013.
- [Stenhammar 13] Joakim Stenhammar, Adriano Tiribocchi, Rosalind J Allen, Davide Marenduzzo & Michael E Cates. *Continuum theory of phase separation kinetics for active Brownian particles*. Physical review letters, vol. 111, no. 14, page 145702, 2013.
- [Tailleur 08] J Tailleur & ME Cates. *Statistical mechanics of interacting run-and-tumble bacteria*. Physical review letters, vol. 100, no. 21, page 218103, 2008.
- [Vicsek 95] Tamás Vicsek, András Czirók, Eshel Ben-Jacob, Inon Cohen & Ofer Shochet. *Novel type of phase transition in a system of self-driven particles*. Physical review letters, vol. 75, no. 6, page 1226, 1995.
- [Vicsek 12] Tamás Vicsek & Anna Zafeiris. *Collective motion*. Physics Reports, vol. 517, no. 3, pages 71–140, 2012.
- [Zwanzig 01] Robert Zwanzig. Nonequilibrium statistical mechanics. Oxford University Press, 2001.